

## Factors Affecting the Seismic Amplification and Bending Moment of Clay-Pile System

S. Banerjee<sup>1</sup>

### ABSTRACT

The response of pile and surrounding soil subjected to earthquake loading is an important factor affecting the integrity of infrastructures. Majority of the research in this field is concentrated to the seismic analysis of piles and pile groups embedded in sand with very few studies conducted involving pile in clay. It is, therefore, well understood that there is a need to study the response of soil-pile system embedded in clay subjected to earthquake loadings. The present paper details the results of numerical simulations carried out for short piles embedded in homogenous clay layer. The study comprises of three major components: (i) Identification of dimensionless groups influencing soil-pile response to seismic shaking (ii) Developing correlations for the maximum bending moment and amplification of seismic waves at the surface of soil and raft and (iii) Comparison of the performance of the developed correlations with the published results.

### Introduction

The response of pile and surrounding soil subjected to earthquake loading is an important factor affecting the integrity of infrastructures. Detailed post earthquake investigations indicated that pile damages during earthquakes are largely influenced by soil-pile interaction. Since early 1970's, several researches were done to account for the inertial and kinematic interaction. Despite this, in the traditional design methods, the pile was designed to carry the flexural stresses arising from the oscillations of the superstructure alone under seismic loading. In this context various analytical, experimental and numerical studies have been conducted to investigate the response of pile subjected to seismic loading. Initially, the researches focused on dynamic response of pile head motion and associated curvatures, so that it can be used as an input for the design of superstructure. Nikolaou et al. (2001) identified that the large pile movements due to liquefaction and lateral spreading resulted in excessive bending and shear forces developed along the pile during the passage of seismic waves through soil. Later it was also noted that the study of internal bending moments and shear also plays an important role in seismic design (Tabesh and Poulos 2007).

Moreover researchers suggested that the response of soil-pile system is generally affected by the soil and pile modulus, the peak ground acceleration, the frequency of base excitation and the superstructure loading (Nikolaou et al., 2001; Tabesh & Poulos, 2007). It was also found that very few studies conducted for pile in clay. However Wilson (1998) noted that the piles in firm cohesionless soils generally perform better during earthquakes than those in soft clay. Hence, there is a need to study the response of soil-pile system embedded in clay subjected to earthquake loadings. The present paper describes the details and results of parametric study carried out for short piles embedded in homogenous clay layer subjected to earthquakes.

---

<sup>1</sup>Assistant Professor, Department of Civil Engineering, IIT Madras, India, [subhadeep@iitm.ac.in](mailto:subhadeep@iitm.ac.in)

## Numerical Simulation of Clay-Pile-Raft System

The pile-raft system, studied in this paper, is embedded in normally consolidated kaolin clay (water content=66%; LL=80%; PL=40%;  $C_c=0.55$ ;  $K=1.36 \times 10^{-8} \text{m/s}$ ) subjected to far-field earthquake motion. The prototype pile-raft system was a  $2 \times 2$  pile-group with a raft ( $12.5 \text{m} \times 7.5 \text{m} \times 0.5 \text{m}$ ) on top (Figure 1). Each pile had a diameter of 0.9m and a length of 13 m. The pile to pile spacing 's' is chosen such that s/d ratios in the direction of shaking were approximately 11.67 and 6.11 along the direction of the seismic excitations.

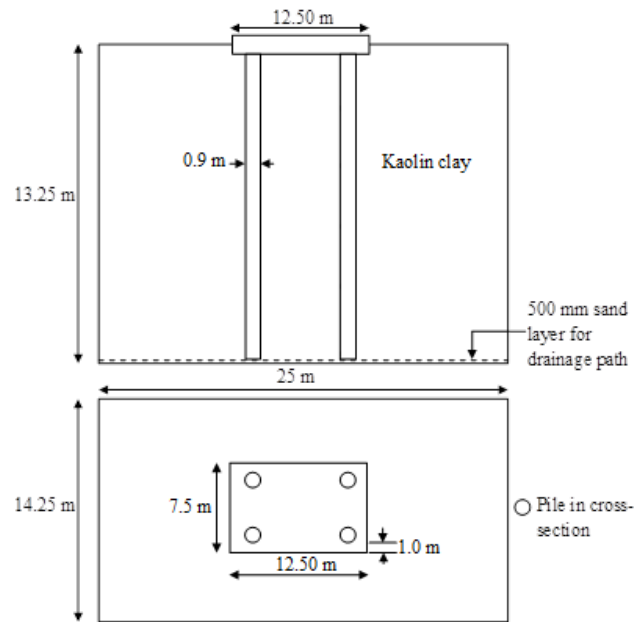


Figure 1. Clay-pile-raft system used for numerical simulations

There are three different types of piles, such as i) hollow stainless steel ( $EI= 354 \text{ MNm}^2$ ), ii) hollow stainless steel filled with PCC ( $EI= 428.50 \text{ MNm}^2$ ) and iii) solid stainless steel ( $EI= 1031 \text{ MNm}^2$ ). The effect of superstructure was considered as additional masses lumped at the raft level. In the following discussions the masses will be termed as, Mass-1 (368 tonnes), Mass-2 (605 tonnes) and Mass-3 (863 tonnes). Three-dimensional finite element analysis of the clay-pile-raft system was carried out using ABAQUS v6.8. By considering the geometry and loading symmetry, half of the prototype was modeled using the 20 noded quadratic brick elements (Figure 2). The input ground motions were applied at the base of the numerical model as prescribed acceleration time histories. The vertical planes of symmetry were restrained in horizontal direction. All the other three vertical faces as well as the base of the model were restrained in vertical direction.

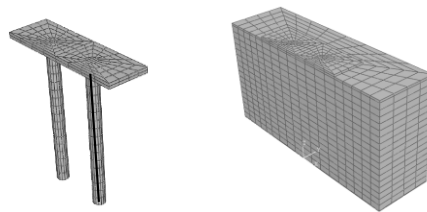


Figure 2. ABAQUS half-model for clay-pile-raft system

Selection of a proper constitutive model for soil is a key issue in numerical modeling of soil-pile interaction. Extensive studies based on both numerical analysis and field monitoring has shown that the degradation of shear modulus with shear strain, or shear stress, significantly influences the performance of a foundation system (Zhu & Chang, 2002). In the present numerical analyses, ABAQUS in-built hypoelastic stress-strain model is used to define the soils that exhibits nonlinear, but reversible, stress strain behavior even at small strains. Physically, the model considers the degradation of shear modulus of soil with respect to increasing strain within the soil mass using Vucetic & Dobry's (1991) design curves for variation of modulus reduction with strain amplitudes for different plasticity index. The earthquake motions considered were the typical far-field events from previous Sumatran earthquakes with long periods and long duration. The input ground motions having identical frequency content and duration were scaled to different peak ground accelerations (PGA) of 0.022g, 0.07g and 0.1g respectively.

Figure 3a and b shows the acceleration time histories computed at the clay surface and top of the raft. For this numerical simulation, solid stainless steel piles with added mass (Mass-3) was used. The model was subjected to the ground motion of PGA-3. By comparing the computed histories at the clay surface and top of the raft with those of the input ground motion, it is clear that amplification of ground motion occurred in both the clay and the structure as the seismic waves propagate upwards. Figure 3c shows the response spectra for the computed histories at the clay and raft along with the response spectra of the input ground motion PGA-3. Figure 3c is replotted in Figure 3d with the amplification of the input ground motion (PGA-3) at the clay surface and top of the raft by normalizing the spectral acceleration at the clay and raft with respect to the base response. Figure shows that the amplifications at the clay surface and top of raft are 1.85 and 1.62 respectively.

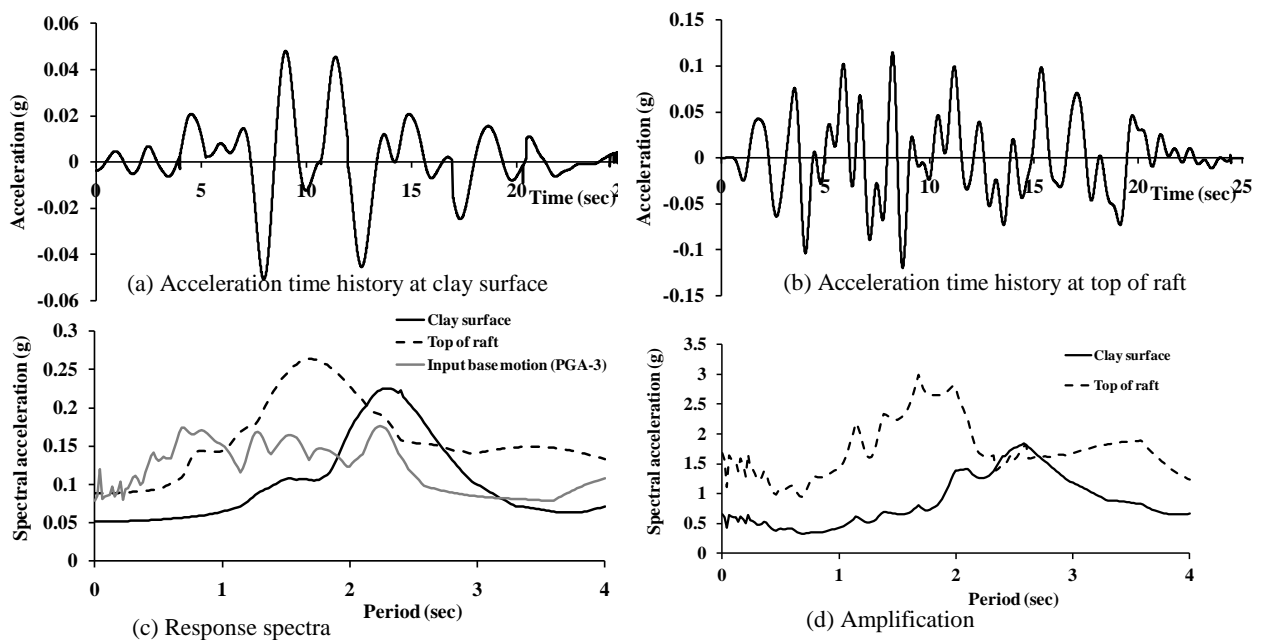


Figure 3. Acceleration time histories, response spectra and amplification computed for solid stainless steel piles with added mass (Mass-3) subjected to the ground motion of PGA-3

To measure the bending moment developed along the pile length, 3-noded quadratic space beam elements (Timoshenko beam element, B32) were introduced along the centerline of the

pile (see Figure 2). The flexural rigidity of the beam was chosen as  $10^6$  times less than that of the pile so that the beam deformed freely without interfering with the structural response of the pile. The actual bending moment was obtained by multiplying computed beam moments by the scaling factor of  $10^6$ . Figure 4 shows the typical maximum bending moment profile plotted along the pile length. The profile shows that the maximum moment occurs near the pile head, and reduces along the pile length to very small value near the pile tip.

### Formulation of Dimensionless Parameters

Review of literature suggests that the response of clay and piles subjected to seismic loading is affected by various factors such as pile modulus, soil modulus, slenderness ratio, natural frequencies of clay layer and pile-raft, superstructure mass, density of the soil and peak ground acceleration (Kavvadas & Gazetas, 1993; Nikolaou et al., 2001; Tabesh & Poulos, 2007; Banerjee, 2007).

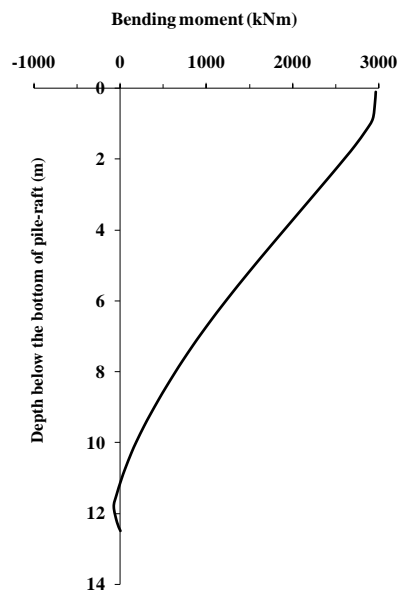


Figure 4. Maximum bending moment profile computed for solid stainless steel piles with added mass (Mass-3) subjected to the ground motion of PGA-3

A total of 27 numerical simulations involving three different pile types, super-structural masses and ground motions were carried out to establish semi-empirical formulations for amplification at clay surface, top of raft and maximum bending moment in pile. In the present study, five dimensionless groups involving different parameters identified are as follows:

(i) Stiffness ratio ( $T_p/T_s$ ) is the ratio of the time period of the superstructure with a superstructure load and without the soil around it to that of the time period of the soil without any superstructure. The pile-raft structure can be considered as a single degree of freedom system where,  $m$  is the mass of the raft, mass of pile is negligible compared to raft and  $(EI)_p$  is flexural rigidity of the pile. Now, stiffness of the system can be worked out from simple structural analysis as,

$$K = \frac{X * (EI)_p}{l_a^3}, \quad (1a)$$

where,  $X$  is a constant whose value depends on the end condition. Hence predominant time period of the superstructure is given by,

$$T_p = 2\pi \sqrt{\frac{m L_p^3}{3 E_p I_p}} \quad (1b)$$

where,  $L_p$  is the length of pile,  $E_p$  is the modulus of elasticity,  $I_p$  is the moment of inertia and  $m$  is the superstructure mass. The time period of the soil layer is given by,

$$T_s = \frac{4h}{\sqrt{\frac{G}{\rho}}} \quad (2)$$

where,  $h$  is the height of the soil layer,  $G$  is the shear modulus of the soil layer and  $\rho$  is the density of the soil layer.

(ii) PGA is the peak ground acceleration of the base excitation expressed in terms of acceleration due to gravity ( $g$ ).

(iii) Mass ratio ( $m/\rho r_p^3$ ) is the ratio of mass of the superstructure to equivalent mass of soil.  $r_p$  is the radius of pile.

(iv) Frequency ratio ( $f_b/f_0$ ) where  $f_b$  is the predominant frequency of the input ground motions and  $f_0 (=1/T_s)$  is the natural frequency of the clay layer.

(v) Slenderness ratio ( $L_p/d$ ) is the ratio of the length of the pile to the diameter of the pile.

### ***Amplification at Clay Surface ( $A_s$ )***

A detail regression analysis shows that the amplification at clay surface can be expressed as an exponential function (Figure 5a) of above mentioned dimensionless groups as shown in Eq. 3a and 3b.

$$A_s = 1.228 \times e^{57802x} \text{ where,} \quad (3a)$$

$$x = \left(\frac{T_p}{T_s}\right)^{0.4} \times (PGA)^7 \times \left(\frac{m}{\rho r_p^3}\right)^{0.05} \times \left(\frac{f_b}{f_0}\right)^{0.6} \quad (3b)$$

It can be noted that the amplification at the clay surface primarily depend on PGA. It is also observed from Eq. 3 that the amplification at the clay surface increases with the decrease in clay stiffness. However one should note that the above formulation is only valid for short piles embedded in clay.

### ***Amplification at Top of Raft ( $A_r$ )***

Amplification at the top of raft is expressed as a function of the amplification at the clay surface. Figure 5b shows the results of the regression analysis as follows,

$$A_r/A_s = 1.991 \times (A_s)^{-0.93} \quad (4)$$

From Eq. 4 it is noted that the amplification at the top of raft increase with the increase in the amplification at the clay surface.

### Maximum Bending Moment developed along the Length of the Pile

In addition to amplifications, the maximum bending moment developed in a pile is also a key parameter for the sustainable design. The maximum moment is represented as a dimensionless formulation,  $Md/E_p I_p$  where  $M$  is the maximum moment,  $d$  is the diameter of the pile,  $E_p I_p$  is the flexural rigidity of the pile. The semi-empirical formulation of the maximum bending moment obtained by regression analysis (Figure 5c) is as follows,

$$\frac{Md}{E_p I_p} = 3 \times 10^{-6} \times \{z\}^{2.545} \quad (5a)$$

$$z = \left(\frac{T_p}{T_s}\right)^{0.4} \times (PGA)^{0.3} \times \left(\frac{m}{\rho r_p^3}\right)^{0.02} \times \left(\frac{f_b}{f_0}\right)^{0.05} \times \left(\frac{L_p}{d}\right)^{0.2} \quad (5b)$$

Eq. 5 suggests that that the stiffness ratio is the main factor affecting the maximum bending moment response of the pile. It also shows that the maximum bending moment increases with the pile modulus, peak ground acceleration and super-structural load. This is in accordance with the findings of Nikolaou et al. (2001), Tabesh and Poulos (2007) and Kang et al. (2012).

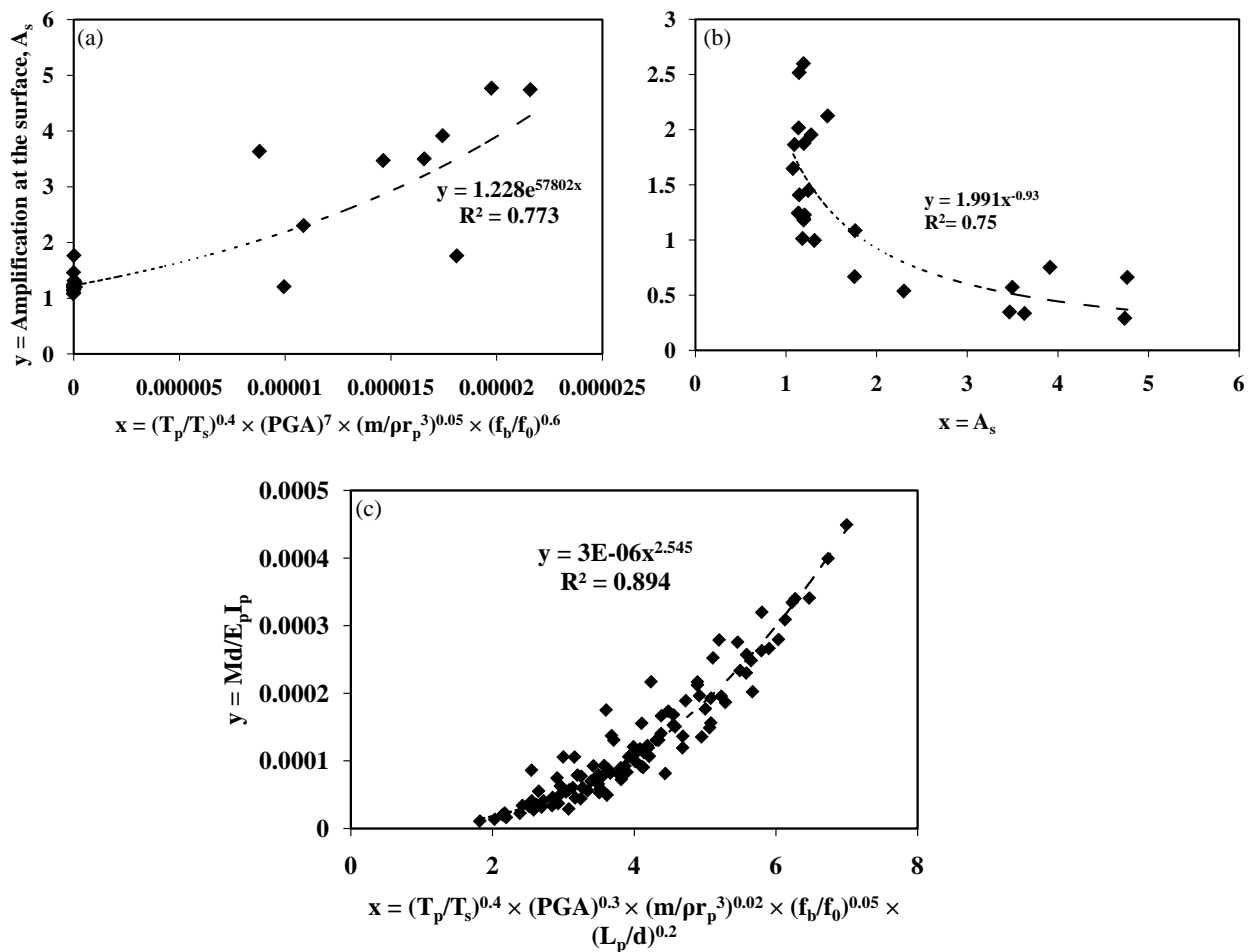


Figure 5. Regression analysis for (a) amplification at clay surface, (b) amplification at the top of the raft, and (c) maximum bending moment

## Validation of the Predictive Relations

Preceding discussion shows that the clay and pile response can be represented as semi-empirical functions of dimensionless groups. The responses computed from the proposed relationships are compared with the results reported in previous studies.

### *Comparison with the Centrifuge Tests Results by Banerjee et al. (2007)*

Banerjee et al. (2007) reported a series of shaking table experiments conducted using geotechnical centrifuge at National University of Singapore. Figure 6a presents the comparison of the results computed from the proposed semi-empirical relationship with the results obtained from the centrifuge tests for the amplification at the clay surface. The figure shows that despite the uncertainties involved in the centrifuge tests, the predicted results matched the test results with reasonable accuracy. Figure 6b shows the comparison between the computed and measured amplifications at the top of raft for different cases. The figure shows that the proposed correlations compares satisfactorily PGA-2 (0.07g) and PGA 3 (0.1g) whereas the centrifuge results obtained from test with ground motion of PGA-1 (0.022g) tends to deviate from the prediction. However the ground motion with PGA of 0.022g may not be a concern in light of amplifications.

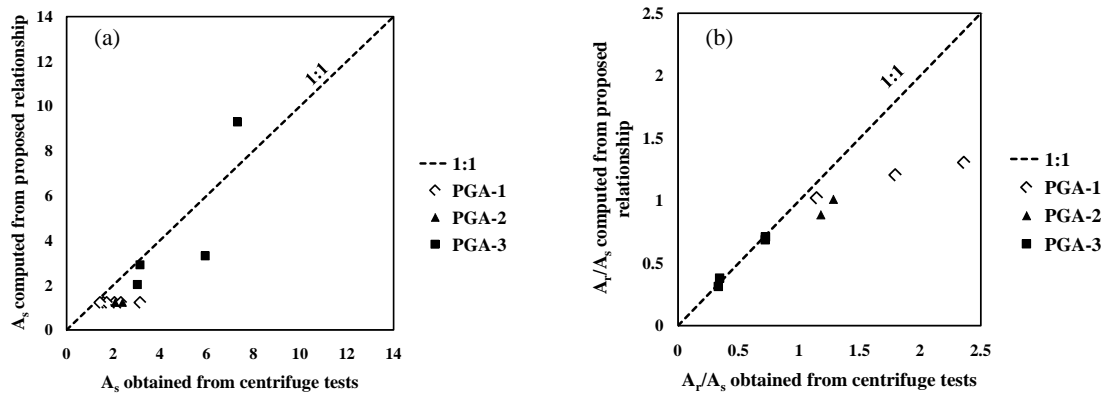


Figure 6. Comparison of amplification at (a) clay surface and (b) top of raft computed from proposed relationship with that obtained from centrifuge tests (Banerjee, 2010)

### *Comparison with the Semi-empirical Relationship proposed by Nikolaou et al. (2001)*

Nikolaou et al. (2001) developed a semi-empirical relationship for maximum bending moment in piles embedded in layered soils as a function of free field acceleration,  $\rho_1$  is the density of soil in layer 1,  $h_1$  is the height of the layer 1,  $l/d$  is the slenderness ratio of the pile,  $E_p$  is the modulus of elasticity of pile,  $E_1$  is the modulus of elasticity of layer 1,  $V_1$  and  $V_2$  are the shear wave velocities of layer 1 & 2 respectively. In the present study, the soil layer is homogenous. Hence,  $V_1/V_2 = 1$  and  $h = 13\text{m}$  (corresponding to the prototype pile length). It can be observed from Figure 7 that the agreement between the proposed correlation and the formulation by Nikolaou et al. (2001) is fairly good. The slight deviations that is observed may be attributed to the effect of superstructure mass, which is not taken into account in the formulation by Nikolaou et al. (2001).

## Conclusion

The foregoing discussion suggests that the response of clay and piles subjected to seismic loading is affected by various factors such as pile modulus, soil modulus, slenderness ratio, natural frequencies of clay layer and pile-raft, superstructure mass, density of the soil and peak ground acceleration. Several major conclusions can be inferred from the present study:

1. The amplification of the ground motion primarily depends on the PGA.
2. An increased amplification at the adjacent clay surface indicates an increased amplification at the top of raft.
3. Flexural rigidity of the pile is the most important factor affecting maximum bending moment. Besides it is also concluded that the maximum bending moment increase with the pile modulus, peak ground acceleration and superstructural load.
4. The developed correlations are favorably validated with the previously published experimental results (Banerjee et al., 2007) as well as the numerical analysis reported by Nikolaou et al. (2001).

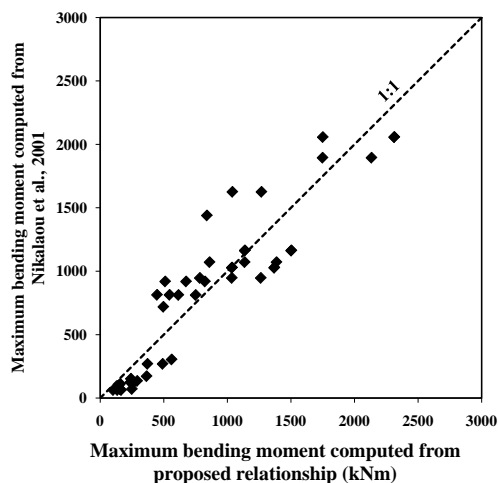


Figure 7. Comparison between bending moments computed using proposed relationship and Nikolaou et al. (2001)

## References

- Banerjee S, Goh S H, Lee F H. Response of soft clay strata and clay-pile-raft systems to seismic shaking. *J Earthquake & Tsunami* 2007; **1**(3): 233 - 255.
- Kang M A, Banerjee S, Lee F H, Xie H P. Dynamic soil-pile-raft interaction in normally consolidated soft clay during earthquakes. *J Earthquake & Tsunami* 2012; **6**(3): 1250031-1 to 31.
- Kavvasdas M, Gazetas G. Kinematic seismic response and bending of free-head piles in layered soil. *Geotechnique* 1993; **43**(2): 207-222.
- Nikolaou S, Mylonakis G, Gazetas G, Tazoh T. Kinematic pile bending during earthquakes: analysis and field measurements. *Geotechnique* 2001; **51**(5): 425-440.
- Tabesh A, Poulos H G. Design charts for seismic analysis of single piles in clay. *Proc ICE (UK) Geotechnical Engineering* 2007; **160** (GE2): 85-96.
- Vucetic M, Dobry R. Effect of soil plasticity on cyclic response. *J Geotech Eng ASCE* 1991; **117**(1): 89-107.
- Wilson D W. *Soil-pile-superstructure interaction in liquefying sand and soft clay*. Ph.D. Thesis 1998.

University of California, Davis, California, USA.

Zhu H, Chang M F. Load transfer curves along bored piles considering modulus degradation. *J Geotech Geoenviron Eng* ASCE 2002; **128**(9): 764-774.